

Article

Visible-Light-Induced, Graphene Oxide-Promoted C3-Chalcogenylation of Indoles Strategy under Transition-Metal-Free Conditions

Qing Huang ¹, Xiangjun Peng ^{2,*}, Hong Li ¹, Haiping He ² and Liangxian Liu ^{1,*}

¹ Department of Chemistry and Chemical Engineering, Gannan Normal University, Ganzhou 341000, China; jxhq6200@163.com (Q.H.); Lihong9600428033@163.com (H.L.)

² Key Laboratory of Prevention and Treatment of Cardiovascular and Cerebrovascular Diseases of Ministry of Education, School of Pharmaceutical Science of Gannan Medical University, Ganzhou 341000, China; hehaiping223@163.com

* Correspondence: pengxiangjun99@126.com (X.P.); liuliangxian1962@163.com (L.L.)

Abstract: An efficient and general method for the synthesis of 3-sulfonylindoles and 3-selenylindoles employing visible-light irradiation with graphene oxide as a promoter at room temperature has been achieved. The reaction features are high yields, simple operation, metal-free and iodine-free conditions, an easy-to-handle oxidant, and gram-scalable synthesis. This simple protocol allows one to access a wide range of 3-arylthioindoles, 3-arylselenylindoles, and even 3-thiocyanatoindoles with good to excellent yields.

Keywords: graphene oxide; visible-light; indole; sulfonylindole; selenylindole



Citation: Huang, Q.; Peng, X.; Li, H.; He, H.; Liu, L. Visible-Light-Induced, Graphene Oxide-Promoted C3-Chalcogenylation of Indoles Strategy under Transition-Metal-Free Conditions. *Molecules* **2022**, *27*, 772. <https://doi.org/10.3390/molecules27030772>

Academic Editor:
Barbara Morzyk-Ociepa

Received: 14 December 2021

Accepted: 19 January 2022

Published: 25 January 2022

Publisher's Note: MDPI stays neutral with regard to jurisdictional claims in published maps and institutional affiliations.



Copyright: © 2022 by the authors. Licensee MDPI, Basel, Switzerland. This article is an open access article distributed under the terms and conditions of the Creative Commons Attribution (CC BY) license (<https://creativecommons.org/licenses/by/4.0/>).

1. Introduction

Organosulfur and organoselenium compounds, which possess broad biological and pharmaceutical activities, have been widely employed as important scaffolds for medicinal chemistry (Figure 1) [1–6]. Among them, 3-sulfonylindoles and 3-selenylindoles represent important classes of sulfur and selenium-containing compounds having more greater therapeutic values in the treatment of cancer [7–12], HIV [13–15], tubulin assembly inhibition [16,17], and bacterial diseases [18–22]. In this regard, numerous methods for the straightforward construction of C-S and C-Se bonds have been developed for the synthesis of 3-sulfonylindoles and 3-selenylindoles. Among these various approaches, the most commonly used methods involved the direct sulfonylation and selenation of the indole moieties with various electrophilic sulfur and selenium reagents [23–35].

However, these strategies suffer from limitations, such as the need for stoichiometric or super stoichiometric amounts of catalysts, strong acidic or oxidizing reagents, harsh reaction conditions, the complex synthetic process of activated sulfur or selenium reagents, and limited substrate scopes [36–41]. Most importantly, these reactions employ arylsulfur or arylselenium reagents such as benzenesulfonyl chlorides [42–45], *N*-(thiophenyl)succinimide [46,47], *S*-phenyl benzenesulfonothioate [48,49], disulfides [50–52], benzene-sulfonhydrazide [53–56], *N*-phenylselenophthalimide [57], *N*-phenylselenosuccinimide [58], and diselenides [59–63], generation of stoichiometric byproducts still cannot be avoided under the conditions used. Therefore, the development of green and sustainable synthetic methods is highly desirable under mild conditions so as to avoid the use of external oxidants, transition metal catalysts, or harsh reaction conditions.

In recent years, graphene oxide (GO) [64–67], which is a readily available and inexpensive material, has historically functioned primarily as a precursor to reduced graphene oxide (rGO) or chemically modified graphene (CMG) materials [68,69], and has generated tremendous excitement due to its potential applications in plastic electronics, solar cells, optical materials, and biosensors [70,71]. In addition, photo-induced organic transformations

have emerged as an attractive and suitable approach in recent years [72–81]. Although GO has been reported as a photocatalyst for hydrogen production from water under UV irradiation [82], the potential application of GO in synthetic photochemistry is still rare [83].

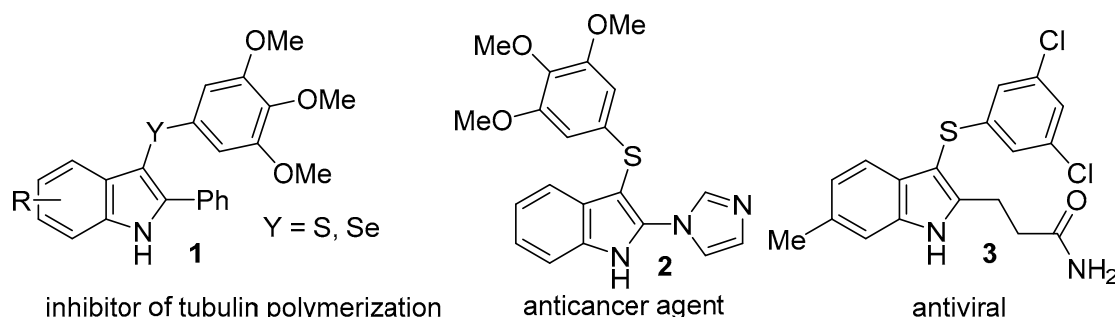
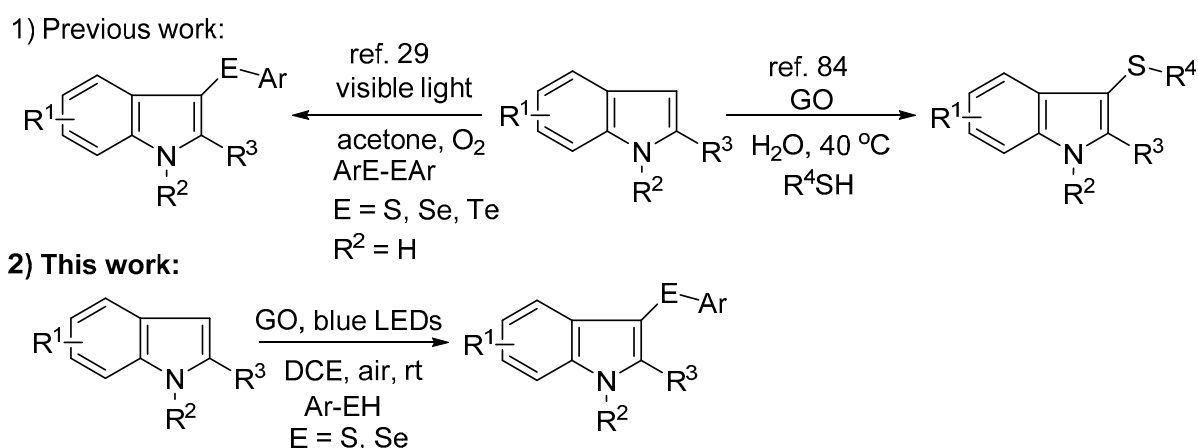


Figure 1. Selected examples of biologically active 3-selanyl- and 3-sulfanylindole compounds.

More recently, Wu et al developed a procedure of GO-mediated thiolation of indoles with thiols in water (Scheme 1) [84]. This methodology provided an atom economical and transition-metal and iodine free procedure for the direct synthesis of 3-sulfenylindoles. Subsequently, Kumar and Rathore reported a benign oxidant, photocatalyst and transition-metal-free visible light induced methodology for the construction of carbon-chalcogen (S, Se, Te) bond that enables the 3-chalcogenyl indole (Scheme 1) [29]. However, most of these methods suffer from some drawbacks such as low atom efficiency and limited substrate scope. Recently, we reported a new and efficient method for the C3-chalcogenylation of indolines employing visible-light irradiation and graphene oxide as a promoter at room temperature [85]. However, the reaction substrates are expensive and difficult to obtain for this synthesis method. In continuation of our work on indole chemistry [86–92] and GO-promoted C-H functionalisation of indoles [93], herein, we wish to report the combination of GO and blue LEDs, which works in synergy to efficiently promote the organo chalcogenylation (S and Se) of indoles in DCE under air atmosphere by using commercially available substrates. The highlight of this work is that GO not only acts as an oxidant, but as a photocatalyst as well.



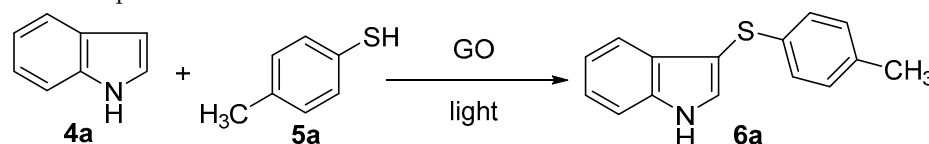
Scheme 1. C3 chalcogenylation of indoles.

2. Results and Discussion

The GO material used in this investigation was prepared by Hummers oxidation of graphite and subsequent exfoliation, as reported [94,95]. The obtained GO material was characterized by X-ray powder diffraction (XRD), transmission electron microscopy (TEM), visible Raman spectroscopy, and atomic force microscopy (AFM) [96] (see the Supplementary Materials).

To commence our investigation, the reaction of indole **4a** with 4-methylbenzenethiol **5a** was performed using 40 wt % GO as a promoter under irradiation with sunlight in open air (Table 1). The reaction proceeded and produced the desired coupling product **6a** with a 28% yield (entry 1). Different light sources, such as CWF bulb (22 W, $\lambda_{\max} = 365 \pm 10$ nm), green LED (1.0 W, $\lambda_{\max} = 530 \pm 10$ nm), and blue LED (3.0 W, $\lambda_{\max} = 425 \pm 15$ nm), were tested. Blue LED was more effective than other light sources, indicating the higher activity of GO in the presence of high-intensity blue light (entries 2–4). The reaction in the absence of a light source either failed to take place at room temperature (entry 5), or only a trace amount of the target product was formed (entry 17). The solvent also plays an important role in this transformation. DCE (1,2-dichloroethane) was more effective than the other tested solvents, such as THF, DMSO, toluene, DMF, and 1,4-dioxane (entries 6–11). Subsequent efforts were directed toward optimizing the GO loadings (entries 12–16). Whereas 50 wt % GO afforded 87% of the target product, decreasing the loading to 20 wt % GO was found to be sufficient to drive the cross-coupling reaction to quantitative conversion. No product was detected without GO. On the basis of our screening experiments, the best reaction condition is using 50 wt % GO in DCE and irradiation with blue LED in open air at 25 °C for 12 h, which afforded the desired product **6a** in high yield (87%, entry 14).

Table 1. Optimization of the reaction conditions ^a.



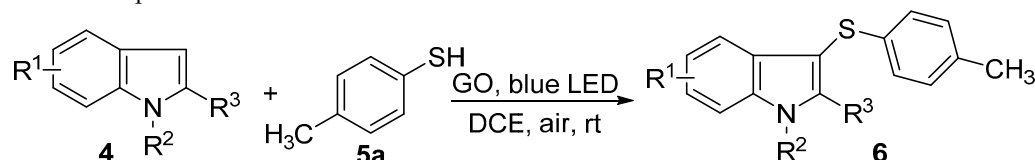
Entry	GO (wt %) ^b	Light Source	Solvent	Yield (%) ^c
1	40	Sunlight	CH ₃ CN	28
2	40	22 W CWF bulb	CH ₃ CN	22
3	40	1W Green LED	CH ₃ CN	7
4	40	3W blue LED	CH ₃ CN	61
5	40	No light	CH ₃ CN	0
6	40	3W blue LED	THF	5
7	40	3W blue LED	DMSO	7
8	40	3W blue LED	Toluene	34
9	40	3W blue LED	DCE	78
10	40	3W blue LED	DMF	0
11	40	3W blue LED	1,4-Dioxane	0
12	20	3W blue LED	DCE	67
13	30	3W blue LED	DCE	72
14	50	3W blue LED	DCE	87
15	60	3W blue LED	DCE	85
16	0	3W blue LED	DCE	0
17	50	No light	DCE	<5

^a Reaction conditions: **4a** (0.3 mmol), **5a** (0.36 mmol), and solvent (1 mL), for 12 h at rt under open air. ^b With respect to the substrate **4a**. ^c Isolated yield.

With the best experimental conditions for the synthesis of **6a** in hand, we first evaluated the efficiency of different substituted indoles **4** while keeping 4-methylbenzenethiol **5a** constant. Under the optimized conditions, the desired products **6aa–6ma** could be efficiently obtained in good to excellent yields (Table 2). Various substituted indoles **4**, i.e., electron-donating (EDG, R = Me, OMe, OBn) and electron-withdrawing (EWG, R = Cl, I,

CN, CO₂CH₃) groups successfully afforded the corresponding 3-sulfenylindoles and had no significant effect on the reactivity and the regioselectivity of reactions. In general, the EDG were better than the EWG. Furthermore, the introduction of various groups at the N-1, C-2, -3, -4, -5, -6, or -7 position of the indoles all proceeded with **5a** under standard reaction conditions. Exceptions to this are 4-methylindole and methyl-4-indolecarboxylate, showing moderate sulfenylation yields (**6ha** and **6ia**), probably due to the steric hindrance effect (entries 8 and 9). Interestingly, introducing a methyl group at the C-3-position of the indole afforded the 2-sulfenylindole product **6ma** in 84% yield.

Table 2. Scope of indoles ^a.

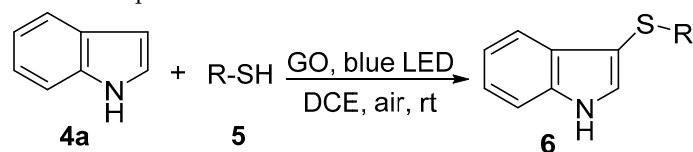


Entry	R ¹	R ²	R ³	Product	Yield (%) ^b
1	H	H	H	6aa	87
2	5-I	H	H	6ba	83
3	5-CH ₃	H	H	6ca	89
4	5-CN	H	H	6da	78
5	6-OCH ₃	H	H	6ea	90
6	7-Cl	H	H	6fa	80
7	7-OBn	H	H	6ga	83
8	4-CH ₃	H	H	6ha	71
9	4-CO ₂ CH ₃	H	H	6ia	67
10	H	H	2-CH ₃	6ja	86
11	H	CH ₃	H	6ka	86
12	5-CH ₃	H	2-CH ₃	6la	82
13 ^c	H	H	3-CH ₃	6ma	84

^a Reaction conditions: **4** (0.3 mmol), **5a** (0.36 mmol), GO (50 wt %) with respect to the substrate **4a**, and DCE (1 mL), for 12 h at rt under open air. ^b Isolated yield. ^c 3-Methyl-2-(*p*-tolylthio)-1*H*-indole (**6ma**) was obtained.

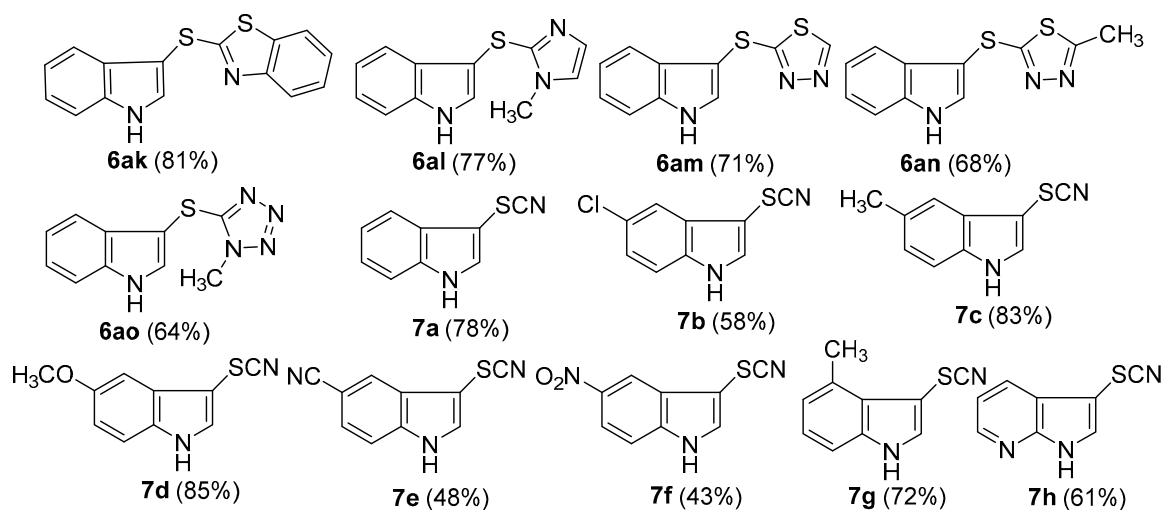
Next, a diverse array of arylthiols were employed as substrates to explore the scope of this reaction (Table 3). These substrates also showed high reactivity in this transformation. All reactions proceeded smoothly when the thiophenol was bearing, regardless of electron-donating groups (Me and OMe) or electron-withdrawing groups (Cl, Br, and NO₂) on the phenyl ring; the 3-sulfenylindoles were obtained in good to excellent yields.

The success in using aryl thiols encouraged us to examine the reaction of indole **4a** with various heterocyclic thiols including benzo[*d*]thiazole-2-thiol, 1-methyl-1*H*-imidazole-2-thiol, 1,3,4-thiadiazole-2-thiol, 5-methyl-1,3,4-thiadiazole-2-thiol, 1-methyl-1*H*-tetrazole-5-thiol, and the results are summarized in Scheme 2. In general, the desired products were formed in moderate to excellent yields under the standard reaction conditions.

Table 3. Scope of thiols ^a.

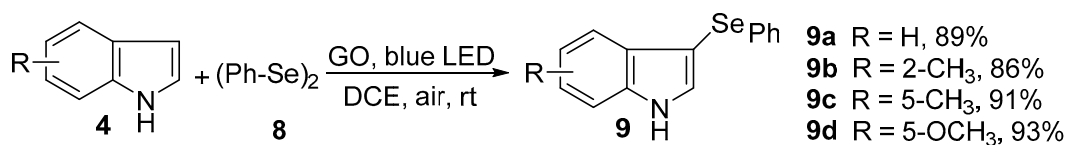
Entry	R	Product	Yield (%) ^b
1	4-CIPh	6ab	86
2	4-BrPh	6ac	88
3	4-OCH ₃ Ph	6ad	83
4	4-C ₂ H ₅ Ph	6ae	80
5	2,4-dimethylphenyl	6af	82
6	4-NO ₂ Ph	6ag	91
7	Naphthalen-2-yl	6ah	78
8 ^c	4-OCH ₃ Ph	6ai	78
9 ^d	4-CH ₃	6aj	76

^a Reaction conditions: 4a (0.3 mmol), 5 (0.36 mmol), GO (50 wt %) with respect to the substrate 4a, and DCE (1 mL), for 12 h at rt under open air. ^b Isolated yield. ^c 5-Methoxy-3-((4-methoxyphenyl)thio)-1H-indole (6ai) was obtained. ^d 3-(*p*-Tolylthio)-1H-pyrrolo[3,2-*b*]pyridine (6aj) was obtained.

**Scheme 2.** Heterocyclic thiols and potassium thiocyanate used as C3 sulfenylation of indoles.

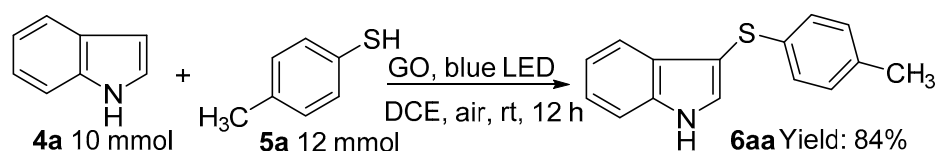
Organothiocyanates are valuable synthetic intermediates which can be easily transformed into an array of organosulfur molecules [97–99]. Under the optimized conditions, we sustained our studies by treating indoles or 1H-pyrrolo[2,3-*b*]pyridine with KSCN under the standard reaction conditions, and the corresponding thiocyanated product 7a–f were obtained with 43–85% yields (Scheme 2). The results have shown that electronegativities of substituents play a major role in governing the reactivity of the substrates. Electron-donating substituents show better results than electron-withdrawing substituents in this transformation.

The developed protocol can also be applied for the preparation of 3-selenyl-indoles using various indole derivatives 4 and diphenyl diselenide 8. In general, the desired products 9 were formed in good to excellent yields in 8 h (Scheme 3), which was more efficient than the generation of 3-sulfenylindoles with regard to the yields and reaction times.



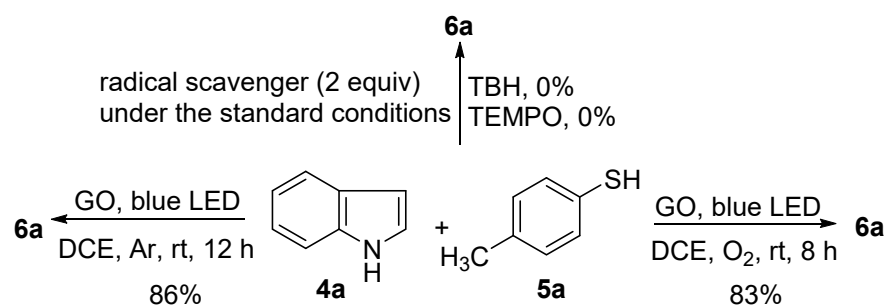
Scheme 3. Synthesis of 3-selenylindoles. Reaction conditions: **4** (0.3 mmol), **8** (0.36 mmol), GO (50 wt %), and DCE (1 mL), for 8 h at rt under open air. Isolated yield.

In order to demonstrate the effectiveness of this new strategy, a gram scale reaction was performed under the standard conditions. 10 mmol indole **4a** and 12 mmol 4-methylbenzenethiol **5a** were subjected to the reaction in the presence of GO (468 mg, 40 wt %) in 50 mL DCE at room temperature. After 12 h, the desired product **6a** was obtained in 84% yield, which demonstrated the practical application of this protocol to prepare 3-sulfenylindoles on a gram-scale (Scheme 4). To our delight, when the amount of GO was reduced to 40 wt %, the yield was not affected to any observable extent.



Scheme 4. Scale-up reaction between **4a** and **5a**.

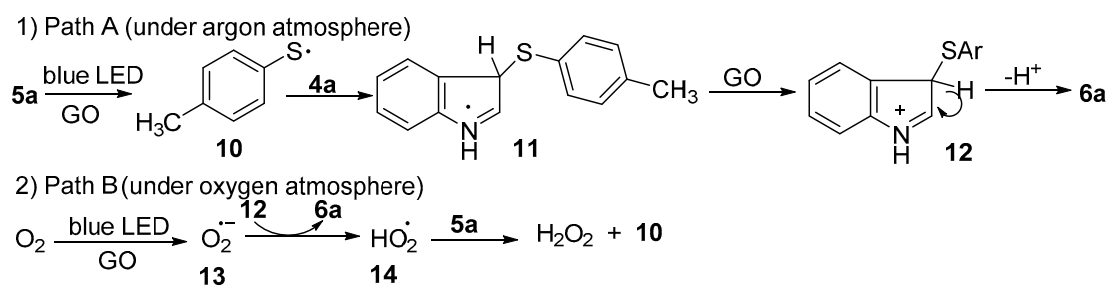
To gain some insight into the mechanism of this reaction, some control experiments were conducted as shown in Scheme 5. Because the visible-light-induced, GO-promoted cross-coupling reaction was performed under open air, the role of O₂ in this reaction was explored. Initially, When the optimal reaction was performed under an oxygen atmosphere instead of open air, there was no effect on the yield, but a faster conversion of the starting material to the reaction product was observed, indicating that O₂ could be involved in the reaction pathway. Similarly, when the reaction was carried out under an argon atmosphere, no major effect was observed, indicating that the reaction follows a different route in an argon environment.



Scheme 5. Control experiments.

Then, radical trapping experiments were conducted by adding butylated hydroxytoluene (BHT) or 2,2,6,6-tetramethyl-1-piperidinyloxy (TEMPO) into the standard conditions of **4a** and **5a**. Experimental results show that these reaction were completely inhibited, indicating the involvement of radical species in the transformation.

On the basis of our control experiments and several other reports from the literature [29,85,100–102], we proposed two plausible mechanisms for this reaction in argon and in oxygen environments as shown in Scheme 6. Graphene oxide might act as a radical initiator [29]. Under an argon atmosphere (path A), promoted by the functional groups on the surface of GO, 5-methylbenzenethiol transformed into phenylthiophenol radical **10**. Next, the thiyl radical **10** interacted with **4a** to produce the radical intermediate **11**. After that, **11** was oxidized to the intermediate **12**. Finally, deprotonation of intermediate **12** led to the formation of product **6a**. GO probably plays a crucial role during the process of oxidation and deprotonation.



Scheme 6. The proposed mechanism for the reaction.

In 2012, Loh et al suggested that the edge sites with unpaired electrons in GO constitute the active catalytic sites and afford enhanced kinetics for the trapping and activation of molecular oxygen by a sequence of electron transport and reduction to superoxide radical [103,104]. Thus, in the case of an oxygen atmosphere (path B), the anion radical of O₂ (O₂^{•−}), which is produced through a SET from unpaired electrons in GO, would abstract a proton from 12, which would generate the desired product 6a and perhydroxyl radical (HO₂[•]). The transfer of H[•] from 5a to HO₂[•] would generate 10 and H₂O₂.

3. Materials and Methods

3.1. General Information

Unless otherwise specified, commercial reagents and solvents were used without further purification. Commercially available chemicals were purchased from Leyan (Shanghai, China) and used without any further purification. ¹H and ¹³C NMR spectra were recorded on a Bruker spectrometer at 400 and 100 MHz, respectively. The chemical shifts were given in parts per million relative to CDCl₃ (7.26 ppm for ¹H) and CDCl₃ (77.0 ppm for ¹³C). Peak multiplicities were reported as follows: s, singlet; d, doublet; t, triplet; m, multiplet; br s, broad singlet and *J*, coupling constant (Hz). Mass spectra were recorded with Bruker Dalton Esquire 3000 plus LC-MS apparatus. Elemental analyses are expressed as percentage values. HRFABMS spectra were recorded on a FTMS apparatus. Silica gel (300–400 mesh) was used for flash column chromatography, eluting (unless otherwise stated) with an ethyl acetate/petroleum ether (PE) (60–90 °C) mixture.

3.2. General Procedure of the Products 6

In a 10 mL Schlenk tube, indole (0.3 mmol), GO (17.6 mg), and thiol (0.36 mmol) were stirred in DCE (1 mL) for 12 h at room temperature under an air atmosphere irradiated by blue LEDs. The reaction mixture was concentrated under reduced pressure. The residue was purified by flash chromatography on silica gel (eluent: EtOAc/PE = 1:10) to yield the corresponding product 6.

3-(*p*-Tolylthio)-1*H*-indole (6aa). Yellow amorphous solid. ¹H NMR (400 MHz, CDCl₃): δ 8.37 (s, 1H), 7.63 (d, *J* = 7.9 Hz, 1H), 7.46 (d, *J* = 2.6 Hz, 1H), 7.43 (d, *J* = 8.1 Hz, 1H), 7.26 (dt, *J* = 1.0, 8.1 Hz, 1H, Ar-H), 7.18 (t, *J* = 7.1 Hz, 1H), 7.05 (d, *J* = 8.3 Hz, 2H), 6.99 (d, *J* = 8.3 Hz, 2H), 2.26 (s, 3H). ¹³C NMR (101 MHz, CDCl₃): δ 136.5, 135.5, 134.7, 130.4, 129.5, 129.1, 126.3, 123.0, 120.8, 119.7, 111.5, 103.6, 20.8. MS (ESI): 240 (M + H⁺, 100). These assignments matched with those previously published [27].

5-Iodo-3-(*p*-tolylthio)-1*H*-indole (6ba). Brown amorphous solid. ¹H NMR (400 MHz, CDCl₃): δ 8.51 (s, 1H, NH), 7.99 (d, *J* = 1.5 Hz, 1H, Ar-H), 7.53 (dd, *J* = 8.5, 1.5 Hz, 1H, Ar-H), 7.43 (d, *J* = 1.5 Hz, 1H, Ar-H), 7.21 (d, *J* = 8.5 Hz, 1H, Ar-H), 7.06–7.01 (m, 4H, Ar-H), 2.29 (s, 3H, CH₃). ¹³C NMR (101 MHz, CDCl₃): δ 135.6, 135.1, 134.9, 131.7, 131.4, 131.3, 129.6, 128.4, 126.3, 113.6, 102.8, 84.6, 20.9. MS (ESI): 366 (M + H⁺, 100). These assignments matched with those previously published [105].

5-Methyl-3-(*p*-tolylthio)-1*H*-indole (6ca). Yellow amorphous solid. ¹H NMR (400 MHz, CDCl₃): δ 8.19 (s, 1H, NH), 7.55 (d, *J* = 0.7 Hz, 1H, Ar-H), 7.40 (d, *J* = 2.6 Hz, 1H, Ar-H), 7.34 (d, *J* = 8.2 Hz, 1H, Ar-H), 7.21–7.13 (m, 3H, Ar-H), 7.08 (d, *J* = 8.2 Hz, 2H, Ar-H), 2.52 (s, 3H, CH₃), 2.36 (s, 3H, CH₃). ¹³C NMR (101 MHz, CDCl₃): δ 135.9, 134.9, 134.7, 130.94,

130.4, 129.7, 129.5, 126.2, 124.7, 119.2, 111.5, 102.4, 21.6, 21.0. MS (ESI): 254 (M + H⁺, 100). These assignments matched with those previously published [105].

3-(*p*-Tolylthio)-1*H*-indole-5-carbonitrile (**6da**). Yellow amorphous solid. ¹H NMR (400 MHz, DMSO-*d*₆): δ 12.20 (s, 1H, NH), 7.99 (d, *J* = 1.6 Hz, 1H, Ar-H), 7.81 (s, 1H, Ar-H), 7.66 (d, *J* = 8.4 Hz, 1H, Ar-H), 7.53 (d, *J* = 8.4 Hz, 1H, Ar-H), 7.04 (d, *J* = 8.0 Hz, 2H, Ar-H), 6.99 (d, *J* = 8.0 Hz, 2H, Ar-H), 2.20 (s, 3H, CH₃). ¹³C NMR (101 MHz, DMSO-*d*₆): δ 139.1, 135.3, 135.2, 134.9, 130.1, 129.0, 126.9, 125.4, 124.1, 120.7, 114.3, 102.8, 102.5, 20.9. MS (ESI): 265 (M + H⁺, 100). These assignments matched with those previously published [106].

6-Methoxy-3-(*p*-tolylthio)-1*H*-indole (**6ea**). Reddish brown amorphous solid. ¹H NMR (400 MHz, CDCl₃): δ 8.33 (s, 1H, NH), 7.51 (d, *J* = 8.6 Hz, 1H, Ar-H), 7.34 (d, *J* = 2.2 Hz, 1H, Ar-H), 7.08 (d, *J* = 8.2 Hz, 2H, Ar-H), 7.02 (d, *J* = 8.2 Hz, 2H, Ar-H), 6.90 (d, *J* = 2.2 Hz, 1H, Ar-H), 6.86 (dd, *J* = 8.6, 2.2 Hz, 1H, Ar-H), 3.87 (s, 3H, OCH₃), 2.29 (s, 3H, CH₃). ¹³C NMR (101 MHz, CDCl₃): δ 157.2, 137.3, 135.6, 134.7, 129.5, 129.3, 126.3, 123.3, 120.3, 110.8, 103.4, 95.2, 55.7, 20.9. MS (ESI): 270 (M + H⁺, 100). These assignments matched with those previously published [106].

7-(Benzyloxy)-3-(*p*-tolylthio)-1*H*-indole (**6ga**). Reddish brown amorphous solid. ¹H NMR (400 MHz, CDCl₃): δ 8.71 (s, 1H, NH), 7.52 (d, *J* = 7.1 Hz, 2H, Ar-H), 7.49–7.40 (m, 4H, Ar-H), 7.27 (d, *J* = 8.4 Hz, 1H, Ar-H), 7.09 (t, *J* = 7.8 Hz, 1H, Ar-H), 7.07 (d, *J* = 8.0 Hz, 2H, Ar-H), 7.01 (d, *J* = 8.0 Hz, 2H, Ar-H), 6.81 (d, *J* = 7.8 Hz, 1H, Ar-H), 5.24 (s, 2H, OCH₂), 2.28 (s, 3H, CH₃). ¹³C NMR (101 MHz, CDCl₃): δ 145.6, 136.9, 135.7, 134.6, 130.8, 130.1, 129.5, 128.7, 128.3, 128.0, 127.2, 126.3, 121.2, 112.6, 104.0, 103.7, 70.4, 20.9. MS (ESI): 346 (M + H⁺, 100). Anal calcd for C₂₂H₁₉NOS: C, 76.49; H, 5.54; N, 4.05; S, 9.28. Found C, 76.35; H, 5.47; N, 4.33; S, 8.95.

4-Methyl-3-(*p*-tolylthio)-1*H*-indole (**6ha**). Reddish brown amorphous solid. ¹H NMR (400 MHz, CDCl₃) δ 8.41 (s, 1H, NH), 7.43 (d, *J* = 2.6 Hz, 1H, Ar-H), 7.29 (d, *J* = 8.1 Hz, 1H, Ar-H), 7.17 (t, *J* = 8.1 Hz, 1H, Ar-H), 7.06–6.98 (m, 4H, Ar-H), 6.92 (d, *J* = 7.1 Hz, 1H), 2.70 (s, 3H, CH₃), 2.29 (s, 3H, CH₃). ¹³C NMR (101 MHz, CDCl₃): δ 137.9, 137.0, 134.3, 132.2, 131.7, 129.6, 127.0, 125.5, 123.1, 122.4, 109.4, 102.9, 20.9, 18.7. MS (ESI): 254 (M + H⁺, 100). These assignments matched with those previously published [106].

Methyl 3-(*p*-tolylthio)-1*H*-indole-4-carboxylate (**6ia**). Brown amorphous solid. ¹H NMR (400 MHz, CDCl₃): δ 9.19 (s, 1H, NH), 7.51 (d, *J* = 2.6 Hz, 1H, Ar-H), 7.49 (d, *J* = 1.0 Hz, 1H, Ar-H), 7.38 (d, *J* = 2.6 Hz, 1H, Ar-H), 7.24 (t, *J* = 7.8 Hz, 1H, Ar-H), 6.98 (s, 4H, Ar-H), 3.68 (s, 3H), 2.30 (d, *J* = 37.7 Hz, 3H). ¹³C NMR (101 MHz, CDCl₃): δ 169.6, 137.6, 136.4, 134.6, 133.4, 129.4, 126.2, 125.4, 125.3, 122.1, 122.0, 115.1, 103.1, 51.9, 20.8. MS (ESI): 298 (M + H⁺, 100). Anal calcd for C₁₇H₁₅NO₂S: C, 68.66; H, 5.08; N, 4.71; S, 10.78. Found C, 68.80; H, 5.26; N, 4.64; S, 10.57.

2-Methyl-3-(*p*-tolylthio)-1*H*-indole (**6ja**). Reddish brown amorphous solid. ¹H NMR (400 MHz, CDCl₃): δ 8.26 (s, 1H, NH), 7.58 (d, *J* = 7.8 Hz, 1H, Ar-H), 7.36 (dt, *J* = 1.0, 7.8 Hz, 1H, Ar-H), 7.22 (dt, *J* = 1.0, 7.8 Hz, 1H, Ar-H), 7.15 (dt, *J* = 1.0, 7.8 Hz, 1H, Ar-H), 6.99 (s, 4H, Ar-H), 2.54 (s, 3H, CH₃), 2.27 (s, 3H, CH₃). ¹³C NMR (101 MHz, CDCl₃): δ 141.0, 135.7, 135.5, 134.4, 130.4, 129.5, 125.8, 122.1, 120.7, 119.0, 110.7, 99.9, 20.9, 12.2. MS (ESI): 254 (M + H⁺, 100). These assignments matched with those previously published [106].

1-Methyl-3-(*p*-tolylthio)-1*H*-indole (**6ka**). Reddish brown amorphous solid. ¹H NMR (400 MHz, CDCl₃): δ 7.75 (d, *J* = 8.2 Hz, 1H, Ar-H), 7.45 (d, *J* = 8.2 Hz, 1H, Ar-H), 7.39 (dt, *J* = 1.0, 7.0 Hz, 1H, Ar-H), 7.37 (s, 1H, Ar-H), 7.28 (dt, *J* = 1.0, 7.0 Hz, 1H, Ar-H), 7.15 (d, *J* = 8.2 Hz, 2H, Ar-H), 7.07 (d, *J* = 8.2 Hz, 1H, Ar-H), 3.86 (s, 3H, NCH₃), 2.35 (s, 3H, CH₃). ¹³C NMR (101 MHz, CDCl₃): δ 137.6, 136.1, 134.9, 134.6, 123.0, 129.6, 126.3, 126.2, 122.6, 120.5, 119.8, 109.8, 101.3, 33.1, 21.0. MS (ESI): 254 (M + H⁺, 100). These assignments matched with those previously published [105].

2,5-Dimethyl-3-(*p*-tolylthio)-1*H*-indole (**6la**). Reddish brown amorphous solid. ¹H NMR (400 MHz, CDCl₃): δ 8.03 (s, 1H, NH), 7.46 (s, 1H, Ar-H), 7.25 (d, *J* = 8.2 Hz, 1H, Ar-H), 7.10 (dd, *J* = 8.2, 1.2 Hz, 1H, Ar-H), 7.46 (s, 4H, Ar-H), 2.51 (s, 3H, CH₃), 2.49 (s, 3H, CH₃), 2.34 (s, 3H, CH₃). ¹³C NMR (101 MHz, CDCl₃): δ 141.3, 136.0, 134.3, 133.8, 130.7,

130.1, 129.6, 125.7, 123.7, 118.7, 110.5, 99.0, 21.5, 20.9, 12.1. MS (ESI): 268 (M + H⁺, 100). These assignments matched with those previously published [106].

3-Methyl-2-(*p*-tolylthio)-1*H*-indole (**6ma**). Reddish brown amorphous solid. ¹H NMR (400 MHz, CDCl₃): δ 7.96 (s, 1H, NH), 7.71 (d, *J* = 7.9 Hz, 1H, Ar-H), 7.33 (d, *J* = 3.6 Hz, 2H, Ar-H), 7.26 (m, 1H, Ar-H), 7.12 (d, *J* = 8.3 Hz, 2H, Ar-H), 7.09 (d, *J* = 8.3 Hz, 2H, Ar-H), 2.51 (s, 3H, CH₃), 2.38 (s, 3H, CH₃). ¹³C NMR (101 MHz, CDCl₃): δ 136.9, 135.9, 133.5, 130.0, 128.6, 127.1, 123.4, 122.3, 119.7, 119.5, 119.4, 111.0, 21.0, 9.6. MS (ESI): 254 (M + H⁺, 100). These assignments matched with those previously published [106].

3-((4-Chlorophenyl)thio)-1*H*-indole (**6ab**). Light yellow amorphous solid. ¹H NMR (400 MHz, CDCl₃): δ 8.47 (s, 1H, NH), 7.58 (d, *J* = 8.0 Hz, 1H, Ar-H), 7.49 (d, *J* = 2.6 Hz, 1H, Ar-H), 7.45 (d, *J* = 8.2 Hz, 1H, Ar-H), 7.29 (dt, *J* = 1.0, 8.0 Hz, 1H, Ar-H), 7.18 (dt, *J* = 1.0, 8.0 Hz, 1H, Ar-H), 7.12 (d, *J* = 8.7 Hz, 2H, Ar-H), 7.02 (d, *J* = 8.7 Hz, 2H, Ar-H). ¹³C NMR (101 MHz, CDCl₃): δ 137.8, 136.5, 130.6, 130.5, 128.7, 128.6, 127.1, 123.1, 121.0, 119.4, 111.6, 102.4. MS (ESI): 260 (M + H⁺, 30), 262 (M + H⁺, 100). These assignments matched with those previously published [105].

3-((4-Bromophenyl)thio)-1*H*-indole (**6ac**). Brown amorphous solid. ¹H NMR (400 MHz, DMSO-*d*₆): δ 11.76 (s, 1H, NH), 7.80 (d, *J* = 2.7 Hz, 1H, Ar-H), 7.51 (d, *J* = 8.1 Hz, 1H, Ar-H), 7.41–7.35 (m, 3H, Ar-H), 7.20 (dt, *J* = 1.1, 8.1 Hz, 1H, Ar-H), 7.08 (dt, *J* = 1.1, 8.1 Hz, 1H, Ar-H), 6.96 (dt, *J* = 2.7, 8.6 Hz, 2H, Ar-H). ¹³C NMR (101 MHz, DMSO-*d*₆): δ 139.5, 137.3, 133.1, 132.1, 128.9, 127.7, 122.7, 120.7, 118.6, 118.0, 112.9, 99.1. MS (ESI): 304 (M + H⁺, 100), 306 (M + H⁺, 100). These assignments matched with those previously published [105].

3-((4-Methoxyphenyl)thio)-1*H*-indole (**6ad**). Brown amorphous solid. ¹H NMR (400 MHz, CDCl₃): δ 8.38 (s, 1H, NH), 7.63 (d, *J* = 8.0 Hz, 1H, Ar-H), 7.46 (d, *J* = 2.6 Hz, 1H, Ar-H), 7.41 (d, *J* = 8.0 Hz, 1H, Ar-H), 7.25 (dt, *J* = 1.0, 8.0 Hz, 1H, Ar-H), 7.17 (dt, *J* = 1.0, 8.0 Hz, 1H, Ar-H), 7.13 (d, *J* = 8.9 Hz, 2H, Ar-H), 6.74 (d, *J* = 8.9 Hz, 2H, Ar-H), 3.73 (s, 3H, OCH₃). ¹³C NMR (101 MHz, CDCl₃): δ 157.8, 136.5, 123.0, 129.5, 129.0, 128.6, 122.9, 120.8, 119.7, 114.5, 111.5, 104.7, 55.3. MS (ESI): 256 (M + H⁺, 100). These assignments matched with those previously published [27].

3-((4-Ethylphenyl)thio)-1*H*-indole (**6ae**). Reddish brown amorphous solid. ¹H NMR (400 MHz, CDCl₃): δ 8.34 (s, 1H, NH), 7.71 (d, *J* = 8.0 Hz, 1H, Ar-H), 7.45 (d, *J* = 2.3 Hz, 1H, Ar-H), 7.44 (d, *J* = 8.0 Hz, 1H, Ar-H), 7.32 (dt, *J* = 1.0, 8.0 Hz, 1H, Ar-H), 7.23 (t, *J* = 7.5 Hz, 1H, Ar-H), 7.13 (d, *J* = 8.2 Hz, 2H, Ar-H), 7.06 (d, *J* = 8.2 Hz, 2H, Ar-H), 2.61 (q, *J* = 7.6 Hz, 2H, CH₂), 1.23 (t, *J* = 7.6 Hz, 3H, CH₃). ¹³C NMR (101 MHz, CDCl₃): δ 141.3, 136.5, 135.9, 130.7, 129.2, 128.5, 126.3, 123.1, 120.9, 119.7, 111.8, 103.2, 28.4, 15.7. MS (ESI): 254 (M + H⁺, 100). Anal calcd for C₁₆H₁₅NS: C, 75.85; H, 5.97; N, 5.53; S, 12.65. Found C, 75.59; H, 5.63; N, 5.71; S, 12.32.

3-((2,4-Dimethylphenyl)thio)-1*H*-indole (**6af**). Tawny amorphous solid. ¹H NMR (400 MHz, CDCl₃): δ 8.28 (s, 1H, NH), 7.71 (d, *J* = 8.0 Hz, 1H, Ar-H), 7.45 (d, *J* = 8.0 Hz, 1H, Ar-H), 7.41 (d, *J* = 2.6 Hz, 1H, Ar-H), 7.36 (t, *J* = 7.7 Hz, 1H, Ar-H), 7.27 (t, *J* = 7.7 Hz, 1H, Ar-H), 7.09 (s, 1H, Ar-H), 6.83 (d, *J* = 8.0 Hz, 1H, Ar-H), 6.78 (d, *J* = 8.0 Hz, 1H, Ar-H), 2.59 (s, 3H, CH₃), 2.34 (s, 3H, CH₃). ¹³C NMR (101 MHz, CDCl₃): δ 136.6, 134.7, 134.6, 134.4, 130.9, 130.5, 129.3, 127.1, 126.1, 123.0, 120.8, 119.7, 111.6, 103.0, 20.7, 19.9. MS (ESI): 254 (M + H⁺, 100). Anal calcd for C₁₆H₁₅NS: C, 75.85; H, 5.97; N, 5.53; S, 12.65. Found C, 76.04; H, 5.83; N, 5.66; S, 12.35.

3-((4-Nitrophenyl)thio)-1*H*-indole (**6ag**). Reddish brown amorphous solid. ¹H NMR (400 MHz, CDCl₃): δ 8.86 (s, 1H, NH), 8.02 (d, *J* = 9.0 Hz, 2H, Ar-H), 7.55 (t, *J* = 7.7 Hz, 1H, Ar-H), 7.54 (d, *J* = 2.6 Hz, 1H, Ar-H), 7.53 (d, *J* = 8.1 Hz, 1H, Ar-H), 7.34 (t, *J* = 8.1 Hz, 1H, Ar-H), 7.22 (t, *J* = 7.7 Hz, 1H, Ar-H), 7.15 (d, *J* = 9.0 Hz, 2H, Ar-H). ¹³C NMR (101 MHz, CDCl₃): δ 150.0, 144.9, 136.7, 131.4, 128.5, 125.2, 123.9, 123.5, 121.4, 119.2, 112.1, 100.1. MS (ESI): 271 (M + H⁺, 100). These assignments matched with those previously published [107].

3-(Naphthalen-2-ylthio)-1*H*-indole (**6ah**). Reddish brown amorphous solid. ¹H NMR (400 MHz, DMSO-*d*₆): δ 11.74 (s, 1H, NH), 7.83 (d, *J* = 2.5 Hz, 1H, Ar-H), 7.77 (d, *J* = 8.6 Hz, 1H, Ar-H), 7.73 (d, *J* = 8.7 Hz, 1H, Ar-H), 7.61 (d, *J* = 7.5 Hz, 1H, Ar-H), 7.50 (d, *J* = 2.6 Hz, 1H, Ar-H), 7.48 (s, 1H, Ar-H), 7.40–7.33 (m, 3H, Ar-H), 7.20 (dd, *J* = 2.6 Hz, 1H, Ar-H), 7.17

(t, $J = 2.6$ Hz, 1H, Ar-H), 7.03 (t, $J = 7.5$ Hz, 1H, Ar-H). ^{13}C NMR (101 MHz, DMSO- d_6): δ 137.3, 137.2, 133.7, 133.0, 131.3, 129.1, 128.8, 128.1, 127.1, 127.0, 125.7, 124.9, 123.3, 122.6, 120.6, 118.8, 112.9, 99.8. MS (ESI): 276 ($M + H^+$, 100). These assignments matched with those previously published [106].

5-Methoxy-3-((4-methoxyphenyl)thio)-1H-indole (**6ai**). Red amorphous solid. ^1H NMR (400 MHz, CDCl_3): δ 8.42 (s, 1H, NH), 7.40 (d, $J = 2.6$ Hz, 1H, Ar-H), 7.28 (d, $J = 8.8$ Hz, 1H, Ar-H), 7.17 (dt, $J = 2.6, 8.8$ Hz, 2H, Ar-H), 7.13 (d, $J = 2.4$ Hz, 1H, Ar-H), 6.95 (dd, $J = 8.8, 2.4$ Hz, 1H, Ar-H), 6.80 (dt, $J = 2.6, 8.8$ Hz, 2H, Ar-H), 3.84 (s, 3H, OCH_3), 3.76 (s, 3H, OCH_3). ^{13}C NMR (101 MHz, CDCl_3): δ 157.8, 155.0, 131.5, 131.0, 129.9, 129.8, 128.3, 114.6, 113.4, 112.5, 103.7, 104.0, 55.9, 55.4. MS (ESI): 286 ($M + H^+$, 100). These assignments matched with those previously published [108].

3-(*p*-Tolylthio)-1H-pyrrolo[3,2-*b*]pyridine (**6aj**). Light yellow amorphous solid. ^1H NMR (400 MHz, DMSO- d_6): δ 11.86 (s, 1H, NH), 8.36 (d, $J = 4.0$ Hz, 1H, Ar-H), 8.00 (d, $J = 2.6$ Hz, 1H, Ar-H), 7.86 (d, $J = 8.1$ Hz, 1H, Ar-H), 7.19 (dd, $J = 8.1, 4.5$ Hz, 1H, Ar-H), 7.00 (d, $J = 7.2$ Hz, 2H, Ar-H), 6.96 (d, $J = 7.2$ Hz, 2H, Ar-H), 2.19 (s, 3H, CH_3). ^{13}C NMR (101 MHz, DMSO- d_6): δ 146.0, 143.8, 136.2, 135.9, 134.5, 129.8, 129.7, 126.5, 120.0, 117.7, 101.6, 20.9. MS (ESI): 241 ($M + H^+$, 100). Anal calcd for $\text{C}_{14}\text{H}_{12}\text{N}_2\text{S}$: C, 69.97; H, 5.03; N, 11.66; S, 13.34. Found C, 70.21; H, 5.37; N, 11.31; S, 13.15.

2-((1H-indol-3-yl)thio)benzo[*d*]thiazole (**6ak**). Brown amorphous solid. ^1H NMR (400 MHz, DMSO- d_6): δ 12.03 (s, 1H, NH), 8.04 (d, $J = 2.8$ Hz, 1H, Ar-H), 7.82 (dd, $J = 2.8, 1.8$ Hz, 1H, Ar-H), 7.80 (dd, $J = 2.1, 1.0$ Hz, 1H, Ar-H), 7.57 (d, $J = 7.8$ Hz, 1H, Ar-H), 7.56 (d, $J = 7.8$ Hz, 1H, Ar-H), 7.41 (dt, $J = 1.2, 8.4$ Hz, 1H, Ar-H), 7.30–7.23 (m, 2H, Ar-H), 7.15 (dt, $J = 1.0, 7.1$ Hz, 1H, Ar-H). ^{13}C NMR (101 MHz, DMSO- d_6): δ 173.8, 154.6, 137.2, 135.4, 134.4, 128.4, 126.6, 124.4, 123.1, 122.1, 121.6, 121.3, 118.5, 113.1, 97.7. MS (ESI): 283 ($M + H^+$, 100). These assignments matched with those previously published [101].

3-((1-Methyl-1H-imidazol-2-yl)thio)-1H-indole (**6al**). Yellow amorphous solid. ^1H NMR (400 MHz, DMSO- d_6): δ 11.51 (s, 1H, NH), 7.69 (s, 1H, Ar-H), 7.60 (d, $J = 7.6$ Hz, 1H, Ar-H), 7.39 (d, $J = 7.6$ Hz, 1H, Ar-H), 7.16 (s, 1H, Ar-H), 7.10 (t, $J = 7.1$ Hz, 1H, Ar-H), 7.04 (t, $J = 7.1$ Hz, 1H, Ar-H), 6.85 (s, 1H, Ar-H), 3.66 (s, 3H, CH_3). ^{13}C NMR (101 MHz, DMSO- d_6): δ 140.0, 136.7, 131.0, 128.9, 128.5, 124.0, 122.4, 120.3, 119.1, 112.5, 100.6, 34.0. MS (ESI): 230 ($M + H^+$, 100). Anal calcd for $\text{C}_{12}\text{H}_{11}\text{N}_3\text{S}$: C, 62.86; H, 4.84; N, 18.33; S, 13.98. Found C, 63.10; H, 5.07; N, 18.05; S, 13.61.

2-((1H-indol-3-yl)thio)-1,3,4-thiadiazole (**6am**). Yellow amorphous solid. ^1H NMR (400 MHz, DMSO- d_6): δ 11.98 (s, 1H, NH), 9.29 (s, 1H, Ar-H), 8.00 (d, $J = 2.8$ Hz, 1H, Ar-H), 7.56 (d, $J = 8.0$ Hz, 1H, Ar-H), 7.53 (d, $J = 7.9$ Hz, 1H, Ar-H), 7.25 (dt, $J = 1.0, 8.0$ Hz, 1H, Ar-H), 7.16 (d, $J = 7.9$ Hz, 1H, Ar-H). ^{13}C NMR (101 MHz, DMSO- d_6): δ 173.0, 154.3, 137.2, 133.6, 127.8, 123.2, 121.3, 118.4, 113.2, 98.6. MS (ESI): 234 ($M + H^+$, 100). Anal calcd for $\text{C}_{10}\text{H}_7\text{N}_3\text{S}_2$: C, 51.48; H, 3.02; N, 18.01; S, 27.48. Found C, 51.83; H, 3.39; N, 17.85; S, 27.17.

2-((1H-indol-3-yl)thio)-5-methyl-1,3,4-thiadiazole (**6an**). Yellow amorphous solid. ^1H NMR (400 MHz, DMSO- d_6): δ 11.95 (s, 1H, NH), 7.96 (d, $J = 2.7$ Hz, 1H, Ar-H), 7.55 (d, $J = 2.7$ Hz, 1H, Ar-H), 7.53 (d, $J = 2.7$ Hz, 1H, Ar-H), 7.24 (d, $J = 7.5$ Hz, 1H, Ar-H), 7.16 (d, $J = 7.5$ Hz, 1H, Ar-H), 2.50 (s, 3H, CH_3). ^{13}C NMR (101 MHz, CDCl_3): δ 172.4, 165.7, 137.1, 133.5, 128.0, 123.1, 121.3, 118.4, 113.1, 98.8, 15.6. MS (ESI): 248 ($M + H^+$, 100). Anal calcd for $\text{C}_{11}\text{H}_9\text{N}_3\text{S}_2$: C, 53.42; H, 3.67; N, 16.99; S, 25.92. Found C, 53.76; H, 3.92; N, 16.84; S, 25.59.

3-((1-Methyl-1H-tetrazol-5-yl)thio)-1H-indole (**6ao**). Pink amorphous solid. ^1H NMR (400 MHz, DMSO- d_6): δ 11.85 (s, 1H, NH), 7.94 (d, $J = 2.7$ Hz, 1H, Ar-H), 7.54 (d, $J = 8.7$ Hz, 1H, Ar-H), 7.51 (d, $J = 8.7$ Hz, 1H, Ar-H), 7.22 (d, $J = 7.2$ Hz, 1H, Ar-H), 7.13 (d, $J = 7.2$ Hz, 1H, Ar-H), 4.03 (s, 3H, NCH_3). ^{13}C NMR (101 MHz, DMSO- d_6): δ 153.8, 136.9, 133.5, 128.8, 122.9, 121.0, 118.6, 112.9, 94.5, 34.5. MS (ESI): 232 ($M + H^+$, 100). Anal calcd for $\text{C}_{10}\text{H}_9\text{N}_5\text{S}$: C, 51.93; H, 3.92; N, 30.28; S, 13.86. Found C, 52.20; H, 4.28; N, 29.91; S, 13.93.

3-Thiocyanato-1H-indole (**7a**). White amorphous solid. ^1H NMR (400 MHz, CDCl_3): δ 8.76 (s, 1H, NH), 7.83 (dd, $J = 5.9, 3.1$ Hz, 1H, Ar-H), 7.52 (d, $J = 2.8$ Hz, 1H, Ar-H), 7.45 (dt, $J = 5.9, 3.1$ Hz, 1H, Ar-H), 7.35 (t, $J = 3.1$ Hz, 1H, Ar-H), 7.33 (t, $J = 3.1$ Hz, 1H, Ar-H). ^{13}C

NMR (101 MHz, CDCl₃): δ 136.0, 131.0, 127.7, 123.9, 121.9, 118.8, 112.1, 111.9, 92.3. MS (ESI): 175 (M + H⁺, 100). These assignments matched with those previously published [109].

5-Chloro-3-thiocyanato-1-*H*-indole (**7b**). Yellow amorphous solid. ¹H NMR (400 MHz, DMSO-*d*₆): δ 12.20 (s, 1H, NH), 8.05 (s, 1H, Ar-H), 7.66 (s, 1H, Ar-H), 7.55 (d, *J* = 7.7 Hz, 1H, Ar-H), 7.26 (d, *J* = 7.7 Hz, 1H, Ar-H). ¹³C NMR (101 MHz, DMSO-*d*₆): δ 135.3, 135.2, 129.1, 126.4, 123.5, 117.4, 115.0, 112.5, 89.9. MS (ESI): 209 (M + H⁺, 100), 211 (M + H⁺, 32). These assignments matched with those previously published [110].

5-Methyl-3-thiocyanato-1-*H*-indole (**7c**). White amorphous solid. ¹H NMR (400 MHz, DMSO-*d*₆): δ 12.00 (s, 1H, NH), 7.94 (d, *J* = 2.9 Hz, 1H, Ar-H), 7.35 (d, *J* = 8.2 Hz, 1H, Ar-H), 7.12 (t, *J* = 8.2 Hz, 1H, Ar-H), 6.93 (d, *J* = 7.1 Hz, 1H, Ar-H), 2.85 (s, 3H, CH₃). ¹³C NMR (101 MHz, DMSO-*d*₆): δ 137.2, 134.6, 129.9, 125.7, 123.4, 123.0, 114.3, 111.3, 89.8, 19.2. MS (ESI): 189 (M + H⁺, 100). These assignments matched with those previously published [111].

5-Methoxy-3-thiocyanato-1-*H*-indole (**7d**). White amorphous solid. ¹H NMR (400 MHz, CDCl₃): δ 8.55 (s, 1H, NH), 7.67 (d, *J* = 8.7 Hz, 1H, Ar-H), 7.40 (d, *J* = 2.7 Hz, 1H, Ar-H), 6.97 (dd, *J* = 8.7, 2.1 Hz, 1H, Ar-H), 6.90 (d, *J* = 2.1 Hz, 1H, Ar-H), 3.86 (s, 3H, OCH₃). ¹³C NMR (101 MHz, CDCl₃): δ 157.7, 136.9, 129.8, 121.8, 119.5, 112.1, 111.9, 95.2, 92.3, 55.7. MS (ESI): 205 (M + H⁺, 100). These assignments matched with those previously published [109].

3-Thiocyanato-1-*H*-indole-5-carbonitrile (**7e**). Yellow amorphous solid. ¹H NMR (400 MHz, DMSO-*d*₆): δ 12.52 (s, 1H, NH), 8.23 (d, *J* = 2.6 Hz, 1H, Ar-H), 8.21 (s, 1H, Ar-H), 7.71 (d, *J* = 8.5 Hz, 1H, Ar-H), 7.64 (dd, *J* = 8.6, 2.6 Hz, 1H, Ar-H). ¹³C NMR (101 MHz, DMSO-*d*₆): δ 143.4, 141.1, 132.5, 130.9, 128.6, 125.1, 119.5, 117.2, 108.7, 96.8. MS (ESI): 200 (M + H⁺, 100). These assignments matched with those previously published [110].

5-Nitro-3-thiocyanato-1-*H*-indole (**7f**). Yellow amorphous solid. ¹H NMR (400 MHz, DMSO-*d*₆): δ 12.63 (s, 1H, NH), 8.51 (d, *J* = 1.8 Hz, 1H, Ar-H), 8.27 (s, 1H, Ar-H), 8.12 (dd, *J* = 9.0, 1.8 Hz, 1H, Ar-H), 7.70 (d, *J* = 9.0 Hz, 1H, Ar-H). ¹³C NMR (101 MHz, DMSO-*d*₆): δ 142.6, 140.0, 137.5, 127.3, 118.6, 114.8, 114.1, 112.4, 93.6. MS (ESI): 220 (M + H⁺, 100). These assignments matched with those previously published [110].

4-Methyl-3-thiocyanato-1-*H*-indole (**7g**). White amorphous solid. ¹H NMR (400 MHz, DMSO-*d*₆): δ 11.91 (s, 1H, NH), 7.92 (d, *J* = 2.9 Hz, 1H, Ar-H), 7.46 (s, 1H, Ar-H), 7.43 (d, *J* = 8.3 Hz, 1H, Ar-H), 7.10 (dd, *J* = 8.3, 1.1 Hz, 1H, Ar-H), 2.45 (s, 3H, CH₃). ¹³C NMR (101 MHz, DMSO-*d*₆): δ 135.1, 133.5, 130.5, 128.2, 125.0, 117.7, 113.0, 112.8, 89.0, 21.6. MS (ESI): 189 (M + H⁺, 100). These assignments matched with those previously published [110].

3-Thiocyanato-1-*H*-pyrrolo[2,3-*b*]pyridine (**7h**). White amorphous solid. ¹H NMR (400 MHz, DMSO): δ 12.62 (s, 1H, NH), 8.40 (d, *J* = 4.5 Hz, 1H, Ar-H), 8.18 (s, 1H, Ar-H), 8.13 (d, *J* = 7.8 Hz, 1H, Ar-H), 7.31 (dd, *J* = 7.8, 4.7 Hz, 1H, Ar-H). ¹³C NMR (101 MHz, DMSO): δ 148.8, 145.0, 134.4, 127.0, 120.3, 117.8, 112.6, 89.5. MS (ESI): 176 (M + H⁺, 100). These assignments matched with those previously published [112].

3-(Phenylselanyl)-1-*H*-indole (**9a**). Yellow amorphous solid. ¹H NMR (400 MHz, CDCl₃): δ 8.43 (s, 1H, NH), 7.69 (d, *J* = 7.9 Hz, 1H, Ar-H), 7.49 (d, *J* = 2.5 Hz, 1H, Ar-H), 7.46 (d, *J* = 8.2 Hz, 1H, Ar-H), 7.33–7.27 (m, 3H, Ar-H), 7.24–7.12 (m, 4H, Ar-H). ¹³C NMR (101 MHz, CDCl₃): δ 136.4, 133.9, 131.3, 130.0, 129.0, 128.7, 125.6, 123.0, 120.9, 120.4, 111.4, 98.2. MS (ESI): 274 (M + H⁺, 100). These assignments matched with those previously published [30].

2-Methyl-3-(phenylselanyl)-1-*H*-indole (**9b**). Yellow amorphous solid. ¹H NMR (400 MHz, CDCl₃): δ 8.20 (s, 1H, NH), 7.64 (d, *J* = 7.7 Hz, 1H, Ar-H), 7.36 (d, *J* = 7.9 Hz, 1H, Ar-H), 7.26 (dd, *J* = 3.5, 1.4 Hz, 1H, Ar-H), 7.23 (dd, *J* = 3.5, 1.4 Hz, 2H, Ar-H), 7.20 (d, *J* = 4.1 Hz, 1H, Ar-H), 7.19–7.12 (m, 3H, Ar-H), 2.56 (s, 3H, CH₃). ¹³C NMR (101 MHz, CDCl₃): δ 141.0, 135.8, 134.0, 131.3, 129.0, 128.4, 125.5, 122.2, 120.7, 119.8, 110.6, 96.2, 13.2. MS (ESI): 288 (M + H⁺, 100). These assignments matched with those previously published [113].

5-Methyl-3-(phenylselanyl)-1-*H*-indole (**9c**). Yellow amorphous solid. ¹H NMR (400 MHz, CDCl₃): δ 8.30 (s, 1H, NH), 7.51 (d, *J* = 0.5 Hz, 1H, Ar-H), 7.44 (d, *J* = 2.5 Hz, 1H, Ar-H), 7.35 (d, *J* = 8.3 Hz, 1H, Ar-H), 7.31–7.28 (m, 2H, Ar-H), 7.22–7.14 (m, 4H, Ar-H), 2.49 (s, 3H, CH₃). ¹³C NMR (101 MHz, CDCl₃): δ 134.7, 134.1, 131.5, 130.4, 130.3, 129.0, 128.6, 125.6, 124.7, 119.9,

111.1, 97.4, 21.5. MS (ESI): 288 (M + H⁺, 100). These assignments matched with those previously published [32].

5-Methoxy-3-(phenylselanyl)-1H-indole (**9d**). Yellow amorphous solid. ¹H NMR (400 MHz, CDCl₃): δ 8.42 (s, 1H, NH), 7.44 (d, *J* = 2.5 Hz, 1H, Ar-H), 7.33 (d, *J* = 8.8 Hz, 1H, Ar-H), 7.30 (dd, *J* = 8.2, 1.5 Hz, 1H, Ar-H), 7.29 (s, 1H, Ar-H), 7.21–7.13 (m, 4H, Ar-H), 6.97 (dd, *J* = 8.8, 2.5 Hz, 1H, Ar-H), 3.85 (s, 3H, OCH₃). ¹³C NMR (101 MHz, CDCl₃): δ 155.1, 134.0, 132.0, 131.4, 130.8, 129.1, 128.5, 125.6, 113.5, 112.4, 101.6, 97.5, 55.9. MS (ESI): 304 (M + H⁺, 100). These assignments matched with those previously published [113].

4. Conclusions

In summary, we have developed a practical GO-promoted and transition metal-free light induced methodology for the construction of a carbon-chalcogen (S and Se) bond that provides 3-chalcogenyl indoles in good to excellent yields under open air. The key features of this simple and robust protocol are: (1) metal-free and iodine-free conditions; (2) easy-to-handle oxidant; (3) open to the air; (4) atom-economic; (5) performed on a gram-scale; (6) regioselective; and (7) applicable to different sources of organochalcogenides with substituted indoles for this transformation. Moreover, very few methods report the combination of GO and light which works in synergy to efficiently promote the organic reactions [83].

Supplementary Materials: The following are available online, Figure S1: (A) SEM image of graphite. (B) SEM image of GO, Figure S2: TEM image of graphite, Figure S3: TEM image of GO, Figure S4: AFM image of GO, Figure S5: Raman image of GO I D /I G ratio = 0.87, Figure S6: XRD image of GO.

Author Contributions: Conceptualization, L.L. and Q.H.; methodology, L.L. and Q.H.; investigation, H.L. and H.H.; writing original draft preparation, X.P.; writing review and editing, L.L.; NMR research, X.P.; supervision, L.L. All authors have read and agreed to the published version of the manuscript.

Funding: This research was funded by National Natural Science Foundation of China (grant number 21462002), Jiangxi Province Office of Education Support Program (grant numbers GJJ190755, GJJ190788), Practice and Innovation Training Program for College Students in Jiangxi Province (grant number 201910413013), Graduate Innovation Project of Gannan Medical University (grant number YC2021-X014), and Fundamental Research Funds for Gannan Medical University (grant number QD202023) for financial support.

Institutional Review Board Statement: Not applicable.

Informed Consent Statement: Not applicable.

Data Availability Statement: Data is contained within the article and Supplementary Material.

Conflicts of Interest: The authors declare that they have no conflict of interest.

Sample Availability: Samples of the compounds **4**, **5**, and **8** are available from the authors.

Electronic Supplementary Information (ESI) Available: Experimental procedures and characterization data, characterization of GO, and ¹H and ¹³C NMR spectra of compounds **6**, **7** and **9**.

References

1. Mellah, M.; Voituriez, A.; Schulz, E. Chiral sulfur ligands for asymmetric catalysis. *Chem. Rev.* **2007**, *107*, 5133–5209. [[CrossRef](#)] [[PubMed](#)]
2. Feng, M.; Tang, B.; Liang, S.; Jiang, X. Sulfur containing scaffolds in drugs: Synthesis and application in medicinal chemistry. *Curr. Top. Med. Chem.* **2016**, *16*, 1200–1216. [[CrossRef](#)] [[PubMed](#)]
3. Jarrett, J.T. The biosynthesis of thiol- and thioether-containing cofactors and secondary metabolites catalyzed by radical S-adenosylmethionine enzymes. *J. Biol. Chem.* **2015**, *290*, 3972–3979. [[CrossRef](#)] [[PubMed](#)]
4. Ostrovidov, S.; Franck, P.; Joseph, D.; Martarello, L.; Kirsch, G.; Belleville, F.; Nabet, P.; Dousset, B. Screening of new antioxidant molecules using flow cytometry. *J. Med. Chem.* **2000**, *43*, 1762–1769. [[CrossRef](#)] [[PubMed](#)]
5. Ninomiya, M.; Garud, D.R.; Koketsu, M. Biologically significant selenium-containing heterocycles. *Coord. Chem. Rev.* **2011**, *255*, 2968–2990. [[CrossRef](#)]
6. Nogueira, C.W.; Rocha, J.B.T. Toxicology and pharmacology of selenium: Emphasis on synthetic organoselenium compounds. *Arch. Toxicol.* **2011**, *85*, 1313–1359. [[CrossRef](#)]

7. Guan, Q.; Han, C.M.; Zuo, D.Y.; Zhai, M.A.; Li, Z.Q.; Zhang, Q.; Zhai, Y.P.; Jiang, X.W.; Bao, K.; Wu, Y.L.; et al. Synthesis and evaluation of benzimidazole carbamates bearing indole moieties for antiproliferative and antitubulin activities. *Eur. J. Med. Chem.* **2014**, *87*, 306–315. [[CrossRef](#)]
8. La Regina, G.; Edler, M.C.; Brancale, A.; Kandil, S.; Coluccia, A.; Piscitelli, F.; Hamel, E.; De Martino, G.; Matesanz, R.; Díaz, J.F.; et al. Arylthioindole inhibitors of tubulin polymerization. 3. Biological evaluation, structure-activity relationships and molecular modeling studies. *J. Med. Chem.* **2007**, *50*, 2865–2874. [[CrossRef](#)]
9. Avis, I.; Martinez, A.; Tauler, J.; Zudaire, E.; Mayburd, A.; Abu-Ghazaleh, R.; Ondrey, F.; Mulshine, J.L. Inhibitors of the arachidonic acid pathway and peroxisome proliferator-activated receptor ligands have superadditive effects on lung cancer growth inhibition. *Cancer Res.* **2005**, *65*, 4181–4190. [[CrossRef](#)]
10. Pang, Y.; An, B.; Lou, L.; Zhang, J.; Yan, J.; Huang, L.; Li, X.; Yin, S. Design, synthesis, and biological evaluation of novel selenium-containing *iso* combretastatins and phenstatins as antitumor agents. *J. Med. Chem.* **2017**, *60*, 7300–7314. [[CrossRef](#)]
11. Plano, D.; Karelia, D.N.; Pandey, M.K.; Spallholz, J.E.; Amin, S.; Sharma, A.K. Design, synthesis, and biological evaluation of novel selenium (Se-NSAID) molecules as anticancer agents. *J. Med. Chem.* **2016**, *59*, 1946–1959. [[CrossRef](#)] [[PubMed](#)]
12. Nedel, F.; Campos, V.F.; Alves, D.; McBride, A.J.A.; Dellagostin, O.A.; Collares, T.; Savegnago, L.; Seixas, F.K. Substituted diaryl diselenides: Cytotoxic and apoptotic effect in human colon adenocarcinoma cells. *Life Sci.* **2012**, *91*, 345–352. [[CrossRef](#)] [[PubMed](#)]
13. La Regina, G.; Coluccia, A.; Brancale, A.; Piscitelli, F.; Gatti, V.; Maga, G.; Samuele, A.; Pannecouque, C.; Schols, D.; Balzarini, J.; et al. Indolylarylsulfones as HIV-1 non-nucleoside reverse transcriptase inhibitors: New cyclic substituents at indole-2-carboxamide. *J. Med. Chem.* **2011**, *54*, 1587–1598. [[CrossRef](#)] [[PubMed](#)]
14. Sancineto, L.; Mariotti, A.; Bagnoli, L.; Marini, F.; Desantis, J.; Iraci, N.; Santi, C.; Pannecouque, C.; Tabarrini, O. Design and synthesis of diselenobisbenzamides (DISeBAs) as nucleocapsid protein 7 (NCp7) inhibitors with anti-HIV activity. *J. Med. Chem.* **2015**, *58*, 9601–9614. [[CrossRef](#)]
15. Ragno, R.; Coluccia, A.; La Regina, G.; De Martino, G.; Piscitelli, F.; Lavecchia, A.; Novellino, E.; Bergamini, A.; Ciaprini, C.; Sinistro, A.; et al. Design, molecular modeling, synthesis, and anti-HIV-1 activity of new indolyl aryl sulfones. Novel derivatives of the indole-2-carboxamide. *J. Med. Chem.* **2006**, *49*, 3172–3184. [[CrossRef](#)]
16. De Martino, G.; Edler, M.C.; La Regina, G.; Coluccia, A.; Barbera, M.C.; Barrow, D.; Nicholson, R.I.; Chiosis, G.; Brancale, A.; Hamel, E.; et al. New arylthioindoles: Potent inhibitors of tubulin polymerization. 2. Structure-activity relationships and molecular modeling studies. *J. Med. Chem.* **2006**, *49*, 947–954. [[CrossRef](#)]
17. Funk, C.D. Leukotriene modifiers as potential therapeutics for cardiovascular disease. *Nat. Rev. Drug Discov.* **2005**, *4*, 664–672. [[CrossRef](#)]
18. Zhang, M.Z.; Chen, Q.; Yang, G.F. A review on recent developments of indole-containing antiviral agents. *Eur. J. Med. Chem.* **2015**, *89*, 421–441. [[CrossRef](#)]
19. Nuth, M.; Guan, H.C.; Zhukovskaya, N.; Saw, Y.L.; Ricciardi, R.P. Design of potent poxvirus inhibitors of the heterodimeric processivity factor required for viral replication. *J. Med. Chem.* **2013**, *56*, 3235–3246. [[CrossRef](#)]
20. Wen, Z.Y.; Xu, J.W.; Wang, Z.W.; Qi, H.; Xu, Q.L.; Bai, Z.S.; Zhang, Q.; Bao, K.; Wu, Y.L.; Zhang, W.G. 3-(3,4,5-Trimethoxyphenylselenenyl)-1*H*-indoles and their selenoxides as combretastatin A-4 analogs: Microwave-assisted synthesis and biological evaluation. *Eur. J. Med. Chem.* **2015**, *90*, 184–194. [[CrossRef](#)]
21. Sahu, P.K.; Umme, T.; Yu, J.; Nayak, A.; Kim, G.; Noh, M.; Lee, J.-Y.; Kim, D.-D.; Jeong, L.S. Selenoacyclovir and selenoganciclovir: Discovery of a new template for antiviral agents. *J. Med. Chem.* **2015**, *58*, 8734–8738. [[CrossRef](#)]
22. Chen, H.X.; Olatunji, O.J.; Zhou, Y.F. Anti-oxidative, anti-secretory and anti-inflammatory activities of the extract from the root bark of *Lycium chinense* (Cortex Lycii) against gastric ulcer in mice. *J. Nat. Med.* **2016**, *70*, 610–619. [[CrossRef](#)] [[PubMed](#)]
23. Yang, F.L.; Tian, S.K. Iodine-catalyzed regioselective sulfenylation of indoles with sulfonyl hydrazides. *Angew. Chem. Int. Ed.* **2013**, *52*, 4929–4932. [[CrossRef](#)] [[PubMed](#)]
24. Thurow, S.; Penteado, F.; Perin, G.; Alves, D.; Santi, C.; Monti, B.; Schiesser, C.H.; Barcellos, T.; Lenardão, E.J. Selenium dioxide-promoted selective synthesis of mono- and bis-sulfenylindoles. *Org. Chem. Front.* **2018**, *5*, 1983–1991. [[CrossRef](#)]
25. Azeredo, J.B.; Godoi, M.; Martins, G.M.; Silveira, C.C.; Braga, A.L. A solvent- and metal-free synthesis of 3-chalcogenyl-indoles employing DMSO/I₂ as an eco-friendly catalytic oxidation system. *J. Org. Chem.* **2014**, *79*, 4125–4130. [[CrossRef](#)]
26. Maeda, Y.; Koyabu, M.; Nishimura, T.; Uemura, S. Vanadium-catalyzed sulfenylation of indoles and 2-naphthols with thiols under molecular oxygen. *J. Org. Chem.* **2004**, *69*, 7688–7693. [[CrossRef](#)]
27. Prasad, C.D.; Kumar, S.; Sattar, M.; Adhikary, A.; Kumar, S. Metal free sulfenylation and bis-sulfenylation of indoles: Persulfate mediated synthesis. *Org. Biomol. Chem.* **2013**, *11*, 8036–8040. [[CrossRef](#)]
28. Rafique, J.; Saba, S.; Franco, M.S.; Bettanin, L.; Schneider, A.R.; Silva, L.T.; Braga, A.L. Direct, meta-free C(sp²)-H chalcogenation of indoles and imidazopyridines with dichalcogenides catalysed by KIO₃. *Chem. Eur. J.* **2018**, *24*, 4173–4180. [[CrossRef](#)]
29. Rathore, V.; Kumar, S. Visible-light-induced metal and reagent-free oxidative coupling of sp² C–H bonds with organo-dichalcogenides: Synthesis of 3-organochalcogenyl indoles. *Green Chem.* **2019**, *21*, 2670–2676. [[CrossRef](#)]
30. Cao, Y.; Liu, J.; Liu, F.M.; Jiang, L.Q.; Yi, W.B. Copper-catalyzed direct and odorless selenylation with a sodium selenite-based reagent. *Org. Chem. Front.* **2019**, *6*, 825–829. [[CrossRef](#)]
31. Luo, D.P.; Wu, G.; Yang, H.; Liu, M.C.; Gao, W.X.; Huang, X.B.; Chen, J.X.; Wu, H.Y. Copper-catalyzed three-component reaction for regioselective aryl- and heteroarylselenation of indoles using selenium powder. *J. Org. Chem.* **2016**, *81*, 4485–4493. [[CrossRef](#)] [[PubMed](#)]

32. Zhang, X.; Wang, C.G.; Jiang, H.; Sun, L.H. Convenient synthesis of selenyl-indoles *via* iodide ion-catalyzed electrochemical C-H selenation. *Chem. Commun.* **2018**, *54*, 8781–8784. [[CrossRef](#)] [[PubMed](#)]
33. Zhang, Q.B.; Ban, Y.L.; Yuan, P.F.; Peng, S.J.; Fang, J.G.; Wu, L.Z.; Liu, Q. Visible-light-mediated aerobic selenation of (hetero)arenes with diselenides. *Green Chem.* **2017**, *19*, 5559–5563. [[CrossRef](#)]
34. Vieira, B.M.; Thurow, S.; da Costa, M.; Casaril, A.M.; Domingues, M.; Schumacher, R.F.; Perin, G.; Alves, D.; Savegnago, L.; Lenard, E.J. Ultrasound-Assisted Synthesis and antioxidant activity of 3-selenyl-1 *H*-indole and 3-selenylimidazo[1,2-*a*]pyridine derivatives. *Asian J. Org. Chem.* **2017**, *6*, 1635–1646. [[CrossRef](#)]
35. Luz, E.Q.; Seckler, D.; Araújo, J.S.; Angst, L.; Lima, D.B.; Rios, E.A.M.; Ribeiro, R.R.; Rampon, D.S. Fe(III)-catalyzed direct C3 chalcogenylation of indole: The effect of iodide ions. *Tetrahedron* **2019**, *75*, 1258–1266. [[CrossRef](#)]
36. Silveira, C.C.; Mendes, S.R.; Wolf, L.; Martins, G.M. The use of anhydrous CeCl₃ as a catalyst for the synthesis of 3-sulfenyl indoles. *Tetrahedron Lett.* **2010**, *51*, 2014–2016. [[CrossRef](#)]
37. Wu, G.; Liu, Q.; Shen, Y.; Wu, W.; Wu, L. Regioselective thiocyanation of aromatic and heteroaromatic compounds using ammonium thiocyanate and oxone. *Tetrahedron Lett.* **2005**, *46*, 5831–5834. [[CrossRef](#)]
38. Ranjit, S.; Lee, R.; Heryadi, D.; Shen, C.; Wu, J.; Zhang, P.; Huang, K.-W.; Liu, X. Copper-mediated C-H activation/C-S cross-coupling of heterocycles with thiols. *J. Org. Chem.* **2011**, *76*, 8999–9007. [[CrossRef](#)]
39. Tudge, M.; Tamiya, M.; Savarin, C.; Humphrey, G.R. Development of a novel, highly efficient halide-catalyzed sulfenylation of indoles. *Org. Lett.* **2006**, *8*, 565–568. [[CrossRef](#)]
40. Khazaei, A.; Zolfigol, M.A.; Mokhlesi, M.; Panah, F.D.; Sajjadifar, S. Simple and highly efficient catalytic thiocyanation of aromatic compounds in aqueous media. *Helv. Chim. Acta* **2012**, *95*, 106–114. [[CrossRef](#)]
41. Silveira, C.C.; Mendes, S.R.; Wolf, L.; Martins, G.M.; von Mühlen, L. Efficient synthesis of 3-selenyl- and 3-sulfanylindoles employing trichloroisocyanuric acid and dichalcogenides. *Tetrahedron* **2012**, *68*, 10464–10469. [[CrossRef](#)]
42. Rahaman, R.; Devi, N.; Bhagawati, J.R.; Barman, P. Microwave-assisted regioselective sulfenylation of indoles under solvent- and metal-free conditions. *RSC Adv.* **2016**, *6*, 18929–18935. [[CrossRef](#)]
43. Chen, M.; Huang, Z.T.; Zheng, Q.Y. Visible light-induced 3-sulfenylation of *N*-methylindoles with arylsulfonyl chlorides. *Chem. Commun.* **2012**, *48*, 11686–11688. [[CrossRef](#)] [[PubMed](#)]
44. Wu, Q.; Zhao, D.; Qin, X.; Lan, J.; You, J. Synthesis of di(hetero)aryl sulfides by directly using arylsulfonyl chlorides as a sulfur source. *Chem. Commun.* **2011**, *47*, 9188–9190. [[CrossRef](#)]
45. Tocco, G.; Begala, M.; Esposito, F.; Caboni, P.; Cannas, V.; Tramontano, E. ZnO-mediated regioselective C-arylsulfonylation of indoles: A facile solvent-free synthesis of 2- and 3-sulfonylindoles and preliminary evaluation of their activity against drug-resistant mutant HIV-1 reverse transcriptases (RTs). *Tetrahedron Lett.* **2013**, *54*, 6237–6241. [[CrossRef](#)]
46. Nalbandian, C.J.; Miller, E.M.; Toenjes, S.T.; Gustafson, J.L. A conjugate Lewis base–Brønsted acid catalyst for the sulfenylation of nitrogen containing heterocycles under mild conditions. *Chem. Commun.* **2017**, *53*, 1494–1497. [[CrossRef](#)]
47. Hostier, T.; Ferey, V.; Ricci, G.; Pardo, D.G.; Cossy, J. TFA-promoted direct C-H sulfenylation at the C₂ position of non-protected indoles. *Chem. Commun.* **2015**, *51*, 13898–13901. [[CrossRef](#)]
48. Wang, F.X.; Zhou, S.D.; Wang, C.; Tian, S.K. *N*-Hydroxy sulfonamides as new sulfenylating agents for the functionalization of aromatic compounds. *Org. Biomol. Chem.* **2017**, *15*, 5284–5288. [[CrossRef](#)]
49. Ravi, C.; Joshi, A.; Adimurthy, S. C₃ sulfenylation of *N*-heteroarenes in water under catalyst-free conditions. *Eur. J. Org. Chem.* **2017**, *2017*, 3646–3651. [[CrossRef](#)]
50. Sang, P.; Chen, Z.; Zou, J. K₂CO₃ promoted direct sulfenylation of indoles: A facile approach towards 3-sulfenylindoles. *Green Chem.* **2013**, *15*, 2096–2100. [[CrossRef](#)]
51. Shi, Q.; Li, P.; Zhang, Y.; Wang, L. Visible light-induced tandem oxidative cyclization of 2-alkynylanilines with disulfides (diselenides) to 3-sulfenyl- and 3-selenylindoles under transition metal-free and photocatalyst-free conditions. *Org. Chem. Front.* **2017**, *4*, 1322–1330. [[CrossRef](#)]
52. Yi, S.; Li, M.; Mo, W.; Hu, X.; Hu, B.; Sun, N.; Jin, L.; Shen, Z. Metal-free, iodine-catalyzed regioselective sulfenylation of indoles with thiols. *Tetrahedron Lett.* **2016**, *57*, 1912–1916. [[CrossRef](#)]
53. Yang, Y.; Zhang, S.; Tang, L.; Hu, Y.; Zha, Z.; Wang, Z. Catalyst-free thiolation of indoles with sulfonyl hydrazides for the synthesis of 3-sulfenylindoles in water. *Green Chem.* **2016**, *18*, 2609–2613. [[CrossRef](#)]
54. Qiu, J.K.; Hao, W.J.; Wang, D.C.; Wei, P.; Sun, J.; Jiang, B.; Tu, S.J. Selective sulfonylation and diazotization of indoles. *Chem. Commun.* **2014**, *50*, 14782–14785. [[CrossRef](#)] [[PubMed](#)]
55. Li, X.; Xu, Y.; Wu, W.; Jiang, C.; Qi, C.; Jiang, H. Copper-catalyzed aerobic oxidative N-S bond functionalization for C-S Bond formation: Regio- and stereoselective synthesis of sulfones and thioethers. *Chem.-Eur. J.* **2014**, *20*, 7911–7915. [[CrossRef](#)]
56. Nookaraju, U.; Begari, E.; Yetra, R.R.; Kumar, P. CeCl₃·7H₂O-NaI promoted regioselective sulfenylation of indoles with sulfonyl-hydrazides. *Chem. Select* **2016**, *1*, 81–85. [[CrossRef](#)]
57. Nicolaou, K.C.; Claremon, D.A.; Barnette, W.E.; Seitz, S.P. *N*-Phenylselenophthalimide (N-PSP) and *N*-phenylselenosuccinimide (N-PSS). Two versatile carriers of the phenylseleno group. Oxyseleation of olefins and a selenium-based macrolide synthesis. *J. Am. Chem. Soc.* **1979**, *101*, 3704–3706. [[CrossRef](#)]
58. Zhao, X.; Yu, Z.; Xu, T.; Wu, P. Novel Brønsted acid catalyzed three-component alkylations of indoles with *N*-phenylselenophthalimide and styrenes. *Org. Lett.* **2007**, *9*, 5263–5266. [[CrossRef](#)]

59. Mohan, B.; Yoon, C.; Jang, S.; Park, K.H. Copper nanoparticles catalyzed Se(Te)-Se(Te) bond activation: A straightforward route towards unsymmetrical organochalcogenides from boronic acids. *ChemCatChem* **2015**, *7*, 405–412. [[CrossRef](#)]
60. Saba, S.; Rafique, J.; Braga, A.L. Synthesis of unsymmetrical diorganyl chalcogenides under greener conditions: Use of an iodine/DMSO system, solvent- and metal-free approach. *Adv. Synth. Catal.* **2015**, *357*, 1446–1452. [[CrossRef](#)]
61. Chatterjee, T.; Ranu, B.C. Solvent-controlled halo-selective selenylation of aryl halides catalyzed by Cu(II) supported on Al₂O₃. A general protocol for the synthesis of unsymmetrical organo mono- and bis-selenides. *J. Org. Chem.* **2013**, *78*, 7145–7153. [[CrossRef](#)] [[PubMed](#)]
62. Becht, J.-M.; Le Drian, C. Formation of carbon-sulfur and carbon-selenium bonds by palladium-catalyzed decarboxylative cross-couplings of hindered 2,6-dialkoxybenzoic acids. *J. Org. Chem.* **2011**, *76*, 6327–6330. [[CrossRef](#)] [[PubMed](#)]
63. Reddy, V.P.; Kumar, A.V.; Swapna, K.; Rao, K.R. Copper oxide nanoparticle-catalyzed coupling of diaryl diselenide with aryl halides under ligand-free conditions. *Org. Lett.* **2009**, *11*, 951–953. [[CrossRef](#)] [[PubMed](#)]
64. Peng, X.J.; Xu, X.Y.; Liu, Q.; Liu, L.X. Graphene oxide and its derivatives: Their synthesis and use in organic synthesis. *Curr. Org. Chem.* **2019**, *23*, 188–204. [[CrossRef](#)]
65. Chua, C.K.; Pumera, M. Carbocatalysis: The state of “metal-free” catalysis. *Chem. Eur. J.* **2015**, *21*, 12550–12562. [[CrossRef](#)] [[PubMed](#)]
66. Navalon, S.; Dhakshinamoorthy, A.; Alvaro, M.; Garcia, H. Carbocatalysis by graphene-based materials. *Chem. Rev.* **2014**, *114*, 6179–6212. [[CrossRef](#)]
67. Dreyer, D.R.; Todd, A.D.; Bielawski, C.W. Harnessing the chemistry of graphene oxide. *Chem. Soc. Rev.* **2014**, *43*, 5288–5301. [[CrossRef](#)] [[PubMed](#)]
68. Su, C.-L.; Loh, K.-P. Carbocatalysts: Graphene oxide and its derivatives. *Acc. Chem. Res.* **2013**, *46*, 2275–2285. [[CrossRef](#)]
69. Coraux, J.; Marty, L.; Bendiab, N.; Bouchiat, V. Functional hybrid systems based on large-area high-quality graphene. *Acc. Chem. Res.* **2013**, *46*, 2193–2201. [[CrossRef](#)]
70. Dreyer, D.R.; Bielawski, C.W. Carbocatalysis: Heterogeneous carbons finding utility in synthetic chemistry. *Chem. Sci.* **2011**, *2*, 1233–1240. [[CrossRef](#)]
71. Dreyer, D.R.; Park, S.; Bielawski, C.W.; Ruoff, R.S. The chemistry of graphene oxide. *Chem. Soc. Rev.* **2010**, *39*, 228–240. [[CrossRef](#)] [[PubMed](#)]
72. Qin, Y.; Zhu, L.; Luo, S. Organocatalysis in inert C-H bond functionalization. *Chem. Rev.* **2017**, *117*, 9433–9520. [[CrossRef](#)] [[PubMed](#)]
73. Romero, N.A.; Nicewicz, D.A. Organic photoredox catalysis. *Chem. Rev.* **2016**, *116*, 10075–10166. [[CrossRef](#)] [[PubMed](#)]
74. Skubi, K.L.; Blum, T.R.; Yoon, T.P. Dual catalysis strategies in photochemical synthesis. *Chem. Rev.* **2016**, *116*, 10035–10074. [[CrossRef](#)]
75. Prier, C.K.; Rankic, D.A.; MacMillan, D.W.C. Visible light photoredox catalysis with transition metal complexes: Applications in organic synthesis. *Chem. Rev.* **2013**, *113*, 5322–5363. [[CrossRef](#)]
76. Hoffmann, N. Photochemical reactions as key steps in organic synthesis. *Chem. Rev.* **2008**, *108*, 1052–1103. [[CrossRef](#)]
77. Colmenares, J.C.; Varma, R.S.; Nair, V. Selective photocatalysis of lignin-inspired chemicals by integrating hybrid nanocatalysis in microfluidic reactors. *Chem. Soc. Rev.* **2017**, *46*, 6675–6686. [[CrossRef](#)]
78. Narayanam, J.M.R.; Stephenson, C.R.J. Visible light photoredox catalysis: Applications in organic synthesis. *Chem. Soc. Rev.* **2011**, *40*, 102–113. [[CrossRef](#)]
79. Ravelli, D.; Dondi, D.; Fagnoni, M.; Albini, A. Photocatalysis. A multi-faceted concept for green chemistry. *Chem. Soc. Rev.* **2009**, *38*, 1999–2011. [[CrossRef](#)]
80. Yoon, T.P.; Ischay, M.A.; Du, J. Visible light photocatalysis as a greener approach to photochemical synthesis. *Nat. Chem.* **2010**, *2*, 527–532. [[CrossRef](#)]
81. Zeitler, K. Photoredox catalysis with visible light. *Angew. Chem. Int. Ed.* **2009**, *48*, 9785–9789. [[CrossRef](#)]
82. Yeh, T.F.; Syu, J.M.; Cheng, C.; Chang, T.H.; Teng, H. Graphite oxide as a photocatalyst for hydrogen production from water. *Adv. Funct. Mater.* **2010**, *20*, 2255–2262. [[CrossRef](#)]
83. Pan, Y.H.; Wang, S.; Kee, C.W.; Dubuisson, E.; Yang, Y.Y.; Loh, K.P.; Tan, C.H. Graphene oxide and Rose Bengal: Oxidative C–H functionalisation of tertiary amines using visible light. *Green Chem.* **2011**, *13*, 3341–3344. [[CrossRef](#)]
84. Chen, M.; Luo, Y.; Zhang, C.; Guo, L.; Wang, Q.T.; Wu, Y. Graphene oxide mediated thiolation of indoles in water: A green and sustainable approach to synthesize 3-sulfenylindoles. *Org. Chem. Front.* **2019**, *6*, 116–120. [[CrossRef](#)]
85. Liu, C.P.; Peng, X.J.; Hu, D.; Shi, F.; Huang, P.P.; Luo, J.J.; Liu, Q.; Liu, L.X. Direct C₃ chalcogenylation of indolines using a graphene oxide-promoted and visible-light-induced synergistic effect. *N. J. Chem.* **2020**, *44*, 17245–17251. [[CrossRef](#)]
86. Liao, H.W.; Peng, X.J.; Hu, D.; Xu, X.Y.; Huang, P.P.; Liu, Q.; Liu, L.X. CoCl₂-promoted TEMPO oxidative homocoupling of indoles: Access to tryptanthrin derivatives. *Org. Biomol. Chem.* **2018**, *16*, 5699–5706. [[CrossRef](#)]
87. Huang, P.P.; Peng, X.J.; Hu, D.; Liao, H.W.; Tang, S.B.; Liu, L.X. Regioselective synthesis of 2,3'-biindoles mediated by an NBS-induced homo-coupling of indoles. *Org. Biomol. Chem.* **2017**, *15*, 9622–9629. [[CrossRef](#)]
88. Yin, B.; Huang, P.P.; Lu, Y.B.; Liu, L.X. TEMPO-catalyzed oxidative homocoupling route to 3,2'-biindolin-2-ones via an indolin-3-one intermediate. *RSC Adv.* **2017**, *7*, 606–610. [[CrossRef](#)]
89. Deng, Z.F.; Peng, X.J.; Huang, P.P.; Jiang, L.L.; Ye, D.N.; Liu, L.X. A multifunctionalized strategy of indoles to C2-quaternary indolin-3-ones via a TEMPO/Pd-catalyzed cascade process. *Org. Biomol. Chem.* **2017**, *15*, 442–448. [[CrossRef](#)]

90. Jiang, L.L.; Peng, X.J.; Huang, P.P.; Chen, Z.W.; Liu, L.X. TEMPO-catalyzed oxidative dimerization and cyanation of indoles for the synthesis of 2-(1H-indol-3-yl)-3-oxoindoline-2-carbonitriles. *Tetrahedron* **2017**, *73*, 1389–1396. [[CrossRef](#)]
91. Lin, F.; Chen, Y.; Wang, B.S.; Qin, W.B.; Liu, L.X. Silver-catalyzed TEMPO oxidative homocoupling of indoles for the synthesis of 3,3'-biindolin-2-ones. *RSC Adv.* **2015**, *5*, 37018–37022. [[CrossRef](#)]
92. Qin, W.B.; Zhu, J.Y.; Kong, Y.B.; Bao, Y.H.; Chen, Z.W.; Liu, L.X. Metal-free (Boc)₂O-mediated C4-selective direct indolation of pyridines using TEMPO. *Org. Biomol. Chem.* **2014**, *12*, 4252–4259. [[CrossRef](#)] [[PubMed](#)]
93. Peng, X.J.; Zeng, Y.; Liu, Q.; Liu, L.X.; Wang, H.S. Graphene oxide as a green carbon material for cross-coupling of indoles with ethers via oxidation and the Friedel-Crafts reaction. *Org. Chem. Front.* **2019**, *6*, 3615–3619. [[CrossRef](#)]
94. Hummers, W.S.; Offeman, R.E. Preparation of graphitic oxide. *J. Am. Chem. Soc.* **1958**, *80*, 1339. [[CrossRef](#)]
95. Primo, A.; Neatu, F.; Florea, M.; Parvulescu, V.; García, H. Graphenes in the absence of metals as carbocatalysts for selective acetylene hydrogenation and alkene hydrogenation. *Nat. Commun.* **2014**, *5*, 5291–5299. [[CrossRef](#)] [[PubMed](#)]
96. Su, C.L.; Tandiana, R.; Balapanuru, J.; Tang, W.; Pareek, K.; Nai, C.T.; Hayashi, T.; Loh, K.P. Tandem catalysis of amines using porous graphene oxide. *J. Am. Chem. Soc.* **2015**, *137*, 685–690. [[CrossRef](#)] [[PubMed](#)]
97. Bayarmagnai, B.; Matheis, C.; Jouvin, K.; Goossen, L.J. Synthesis of difluoromethyl thioethers from difluoromethyl trimethylsilane and organothiocyanates generated in situ. *Angew. Chem. Int. Ed.* **2015**, *54*, 5753–5756. [[CrossRef](#)]
98. Zhang, Z.H.; Liebeskind, L.S. Palladium-catalyzed, copper(I)-mediated coupling of boronic acids and benzylthiocyanate. A cyanide-free cyanation of boronic acids. *Org. Lett.* **2006**, *8*, 4331–4333. [[CrossRef](#)]
99. Exner, B.; Bayarmagnai, B.; Jia, F.; Goossen, L.J. Iron-catalyzed decarboxylation of trifluoroacetate and its application to the synthesis of trifluoromethyl thioethers. *Chem.-Eur. J.* **2015**, *21*, 17220–17223. [[CrossRef](#)]
100. Saba, S.; Rafique, J.; Franco, M.S.; Schneider, A.R.; Espíndola, L.; Silva, D.O.; Braga, A.L. Rose Bengal catalysed photo-induced selenylation of indoles, imidazoles and arenes: A metal free approach. *Org. Biomol. Chem.* **2018**, *16*, 880–885. [[CrossRef](#)]
101. Saima, E.D.; Lavekar, A.G.; Sinha, A.K. Cooperative catalysis by bovine serum albumin-iodine towards cascade oxidative coupling-C(sp²)-H sulfenylation of indoles/hydroxyaryls with thiophenols on water. *Org. Biomol. Chem.* **2016**, *14*, 6111–6118. [[CrossRef](#)] [[PubMed](#)]
102. Guo, W.; Tan, W.; Zhao, M.; Tao, K.; Zheng, L.Y.; Wu, Y.; Chen, D.; Fan, X.L. Photocatalytic direct C–S bond formation: Facile access to 3-sulfonylindoles via metal-free C-3 sulfenylation of indoles with thiophenols. *RSC Adv.* **2017**, *7*, 37739–37742. [[CrossRef](#)]
103. Su, C.L.; Acik, M.; Takai, K.; Lu, J.; Hao, S.J.; Zheng, Y.; Wu, P.P.; Bao, Q.L.; Enoki, T.; Chabal, Y.J.; et al. Probing the catalytic activity of porous graphene oxide and the origin of this behaviour. *Nat. Commun.* **2012**, *3*, 1298–1306. [[CrossRef](#)] [[PubMed](#)]
104. Lv, G.Q.; Wang, H.L.; Yang, Y.G.; Deng, T.S.; Chen, C.M.; Zhu, Y.L.; Hou, X.L. Graphene oxide: A convenient metal-free carbocatalyst for facilitating aerobic oxidation of 5-hydroxymethylfurfural into 2,5-diformylfuran. *ACS Catal.* **2015**, *5*, 5636–5646. [[CrossRef](#)]
105. Kumaraswamy, G.; Rajua, R.; Narayanarao, V. Metal- and base-free syntheses of aryl/alkylthioindoles by the iodine-induced reductive coupling of aryl/alkyl sulfonyl chlorides with indoles. *RSC Adv.* **2015**, *5*, 22718–22723. [[CrossRef](#)]
106. Yang, X.Q.; Bao, Y.H.; Dai, Z.H.; Zhou, Q.F.; Yang, F.L. Catalyst-free sulfenylation of indoles with sulfinic esters in ethanol. *Green Chem.* **2018**, *20*, 3727–3731. [[CrossRef](#)]
107. Fang, X.L.; Tang, R.Y.; Zhong, P.; Li, J.H. Iron-catalyzed sulfenylation of indoles with disulfides promoted by a catalytic amount of iodine. *Synthesis* **2009**, *24*, 4183–4189. [[CrossRef](#)]
108. Ackermann, L.; Dell'Acqua, M.; Fenner, S.; Vicente, R.; Sandmann, R. Metal-free direct arylations of indoles and pyrroles with diaryliodonium salts. *Org. Lett.* **2011**, *13*, 2358–2360. [[CrossRef](#)]
109. Zhang, X.; Wang, C.G.; Jiang, H.; Sun, L.H. A low-cost electrochemical thio- and selenocyanation strategy for electron-rich arenes under catalyst- and oxidant-free conditions. *RSC Adv.* **2018**, *8*, 22042–22045. [[CrossRef](#)]
110. Li, C.Q.; Long, P.L.; Wu, H.P.; Yin, H.Q.; Chen, F.X. N-Thiocyanato-dibenzenesulfonimide: A new electrophilic thiocyanating reagent with enhanced reactivity. *Org. Biomol. Chem.* **2019**, *17*, 7131–7134. [[CrossRef](#)] [[PubMed](#)]
111. Jiang, H.F.; Yu, W.T.; Tang, X.D.; Li, J.X.; Wu, W.Q. Copper-catalyzed aerobic oxidative regioselective thiocyanation of aromatics and heteroaromatics. *J. Org. Chem.* **2017**, *82*, 9312–9320. [[CrossRef](#)]
112. Wu, D.; Qiu, J.S.; Karmaker, P.G.; Yin, H.Q.; Chen, F.X. N-Thiocyanatosaccharin: A “sweet” electrophilic thiocyanation reagent and the synthetic applications. *J. Org. Chem.* **2018**, *83*, 1576–1583. [[CrossRef](#)]
113. Yu, Y.Z.; Zhou, Y.; Song, Z.Q.; Liang, G. An efficient *t*-BuOK promoted C₃-chalcogenylation of indoles with dichalcogenides. *Org. Biomol. Chem.* **2018**, *16*, 4958–4962. [[CrossRef](#)]